Simultaneous Information and Power Transfer Using Magnetic Resonance

Kisong Lee and Dong-Ho Cho

To deal with the major challenges of embedded sensor networks, we consider the use of magnetic fields as a means of reliably transferring both information and power to embedded sensors. We focus on a power allocation strategy for an orthogonal frequency-division multiplexing system to maximize the transferred power under the required information capacity and total available power constraints. First, we consider the case of a co-receiver, where information and power can be extracted from the same signal. In this case, we find an optimal power allocation (OPA) and provide the upper bound of achievable transferred power and capacity pairs. However, the exact calculation of the OPA is computationally complex. Thus, we propose a low-complexity power reallocation algorithm. For practical consideration, we consider the case of a separated receiver (where information and power are transferred separately through different resources) and propose two heuristic power allocation algorithms. Through simulations using the Agilent Advanced Design System and Ansoft High Frequency Structure Simulator, we validate the magnetic-inductive channel characteristic. In addition, we show the performances of the proposed algorithms by providing achievable η-C regions.

Keywords: Magnetic induction communication, wireless power transfer, embedded sensor networks.

Manuscript received Feb. 6, 2014; revised Aug. 21, 2014 accepted Aug. 28, 2014.

This research was funded by the MSIP (Ministry of Science, ICT & Future Planning), Rep. of Korea in the ICT R&D Program 2014.

Kisong Lee (corresponding author, kslee851105@gmail.com) is with the IT Convergence Technology Research Laboratory, ETRI, Daejeon, Rep. of Korea.

Dong-Ho Cho (dhcho@ee.kaist.ac.kr) is with the Department of Electrical Engineering, KAIST, Daejeon, Rep. of Korea.

I. Introduction

Sensors can be embedded in a wide range of dense media, including water, soils, and masonry walls, which can be used in many applications, such as home networks and underground sensor networks. Sensors for use in home networks can also be embedded in the walls of buildings for the purposes of convenience and aesthetics [1]. Furthermore, sensors can be buried underground to monitor soil conditions or to provide information about earth movements [2]. However, the embedding of sensors presents two main challenges: effective communication between sensors and practical power supply. Therefore, a solution is needed to deal with these obstacles so that, in real-life practices, embedded sensors can operate more effectively and for longer periods of time.

Magnetic induction (MI) communication is emerging as a promising technology that can allow embedded sensors to communicate with each other. Traditionally, wireless communications have relied on the use of electromagnetic (EM) radiation. However, EM waves are not appropriate for the transfer of information in dense media due to the three major problems of high path loss, dynamic channel variation, and large antenna size [3]–[4]. On the other hand, MI communication uses the MI of coil antennas to transfer information. The magnetic permeability of media such as water or soil is similar to that of air [2]. This means that magnetic fields experience a lower propagation loss than EM waves in dense media. Therefore, magnetic fields are more appropriate than EM waves as a mechanism of communication for embedded sensor networks. Recently, many research groups are actively investigating MI communication, including path loss, capacity, and MI waveguide techniques [2]–[10].

Batteries are not a suitable power source for embedded

http://dx.doi.org/10.4218/etrij.14.0114.0161

sensors because their replacement is unlikely to be straightforward. One solution is the wireless transfer of power, an established technology that can be used to eliminate the need for a wired power connection. The efficient transfer of power is possible over a range of several meters using coupled magnetic resonance [11]–[18].

Both MI communication and wireless power transfer can be achieved using magnetic fields. Therefore, it should be possible to transfer both information and power simultaneously through magnetic fields. To maximize the transfer of power, it is best to use one sinusoid at the resonant frequency that has the highest power transfer efficiency. However, a sinusoid with a bandwidth of zero has a communication capacity of zero. Therefore, there is a trade-off between communication capacity and power transfer efficiency, with respect to bandwidth. However, the following works considered EM waves as the means for transferring information and power, not magnetic fields; as a result, the properties of magnetic-inductive channels were not reflected [19]–[21].

In this paper, we consider the simultaneous optimization of information and power transfer so as to enable the practical use of embedded sensors. In practice, a low data rate is generally satisfactory for the transfer of information in embedded sensor networks [2]. On the other hand, for the successful operation of sensors, it is important to ensure a stable power supply. Therefore, our approach is focused on maximizing the transferred power, while ensuring the required information capacity. Our contributions can be described as follows. First, we present a magnetic-inductive channel model and a wireless information and power transfer system. We also verify the characteristics of the magnetic-inductive channel using the Agilent Advanced Design System (ADS) and the Ansoft High Frequency Structure Simulator (HFSS). Based on the optimization problem, we consider the case of a co-receiver (where information and power are transferred simultaneously through the same resource) to obtain the upper bound of achievable transferred power and capacity pairs. Here, we use an optimization technique to find the optimal allocated power, which is found by adjusting the water level of each subchannel. We also derive the conditions for the existence and boundedness of the optimal solution. The calculation of the optimal power allocation (OPA) is computationally complex. So, we propose a low-complexity power reallocation algorithm, which finds a near-OPA with a reduced computational complexity. However, it is difficult in practice to implement in the case of a co-receiver. Thus, we consider only the case of a separated receiver, where information and power are transferred separately through different resources. In this case, we propose two heuristic power allocation algorithms — one based on frequency division and the other on time division. We also describe the η-C regions, which show the achievable power transfer efficiency and information capacity. Here, we compare the performance of the proposed algorithms with that of the optimal solution and that of a conventional equal power allocation. Carrying out simulations, we show that the proposed algorithms have a significant performance gain with respect to power transfer efficiency.

II. System Model and Magnetic-Inductive Channel

A block diagram that illustrates our wireless information and power transfer system using magnetic resonance is shown in Fig. 1. Here, r_t and r_r are the radii of the transmitter coil (Tx coil) and receiver coil (Rx coil), respectively. The two coils lie along a single axis and are separated by a distance, d. Also, Fig. 1 shows its equivalent circuit model, which contains the effect of inductive coupling between the two coils. The Tx coil is connected to an alternating voltage source, V_S, with an angular frequency, ω. The Rx coil is connected to the load resistance, R_L. The self-inductances of the Tx and Rx coils are L_t and L_r, respectively; r_{lt} and r_{lr} are the internal resistances of the coils; and C_t and C_r are the capacitances that make the two coils resonate at the same resonant frequency. The angular resonant frequency ω_o can be defined as follows:

$$\omega_o = 2\pi f_c = \frac{1}{\sqrt{L_t C_t}} = \frac{1}{\sqrt{L_r C_r}}, \quad (1)$$

where f_c is a resonant frequency. In the Tx coil, a sinusoidal current, $i_t(\omega)$, is generated by the voltage source V_S. Then, $i_t(\omega)$ induces another sinusoidal current, $i_r(\omega)$, in the Rx coil. This implies that the wireless link between the two coils is generated through inductive coupling. And, this mechanism makes it possible to transfer information and power wirelessly. The MI between the coils can be represented by the following coupling coefficient, k, such that $k = M/(L_t L_r)^{1/2}$, where M is the mutual

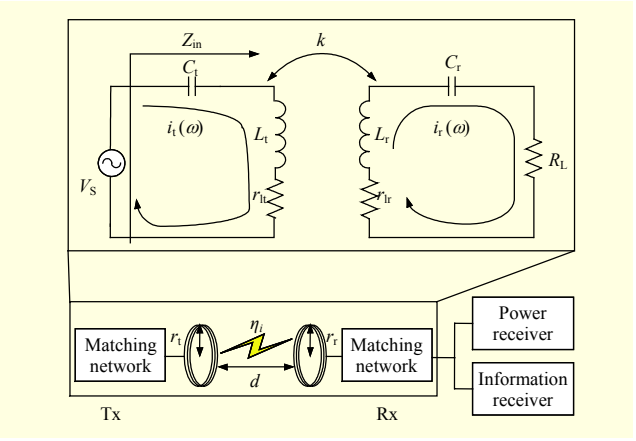

Fig. 1. Wireless information and power transfer system.

inductance. Also, k can be approximated as a function of the distance between the coils [8], as follows:

$$k(d) = \frac{r_t^2 r_r^2}{\sqrt{r_t r_r}(\sqrt{d^2 + r_t^2})^3}. \quad (2)$$

In addition, we consider a multicarrier-based wireless information and power transfer system, such as an orthogonal frequency-division multiplexing (OFDM) system [22]. In this system, the resonant frequency is used as a central frequency for the transfer of information, and the total bandwidth of the frequency band is B. This frequency band is divided into N subchannels, each of which has the same bandwidth size (B/N).

Using the equivalent circuit model, we can derive the equivalent input impedance Z_{in}, which reflects the effect of coupling seen in the Tx coil.

$$Z_{in} = r_{lt} + j\omega L_t + 1/j\omega C_t + \frac{k^2\omega^2 L_t L_r}{r_{lr} + j\omega L_r + 1/j\omega C_r + R_L}. \quad (3)$$

Here, we define the function $f(\omega)$ for the Tx coil as $f(\omega) = j\omega L_t + 1/j\omega C_t$; then, the first derivation of $f(\omega)$ is obtained as $f'(\omega) = j(L_t + 1/\omega^2 C_t)$. Using the first-order Taylor series expansion, $f(\omega)$ near ω_o can be approximated as follows:

$$\begin{aligned} f(\omega) &= f(\omega_o) + f'(\omega_o)(\omega - \omega_o) \\ &= 0 + j(L_t + \frac{1}{\omega_o^2 C_t})(\omega - \omega_o) \\ &= j2(\frac{\omega - \omega_o}{\omega_o})(\frac{\omega_o L_t}{r_{lt}})r_{lt} \\ &= j2(\Delta\omega)(Q_t)r_{lt}, \end{aligned} \quad (4)$$

where the quality factor of Tx, $Q_t = \omega_o L_t / r_{lt}$, denotes the strength of the mutual coupling near the resonant frequency. Using a similar method to that used in obtaining (4), the quality factor of Rx can be found as $Q_r = \omega_o L_r / r_{lr}$. Then, Z_{in} can be approximated as

$$\begin{aligned} Z_{in} &= r_{lt}(1 + j2\Delta\omega Q_t) + \frac{k^2\omega^2 L_t L_r}{r_{lr}(1 + j2\Delta\omega Q_r) + R_L} \\ &= Z_{in,1} + Z_{in,2}. \end{aligned} \quad (5)$$

From (5), the power transfer efficiency (PTE) at a frequency of ω can be expressed as

$$\begin{aligned} \eta_\omega &= \frac{Z_{in,2}}{Z_{in,1} + Z_{in,2}} \times \frac{R_L}{r_{lr}(1 + j2\Delta\omega Q_r) + R_L} \\ &= \frac{1}{\left[1 + \frac{Q_L(1 + j2\Delta\omega Q_r)}{Q_r}\right]\left[1 + \frac{1}{\sigma^2}\left(1 + \frac{Q_r}{Q_L(1 + j2\Delta\omega Q_r)}\right)^2\right]}. \end{aligned} \quad (6)$$

Here, $Q_L = \omega_o L_r / R_L$ and σ are the distance-dependent figure of merit (FOM), which are defined as follows:

$$\sigma = k\sqrt{\frac{Q_t Q_r}{(1 + j2\Delta\omega Q_t)(1 + j2\Delta\omega Q_r)}}. \quad (7)$$

Substituting (2) and (7) into (6), we can see that η_ω is proportional to $1/d^6$ as the path loss of the MI channel for communication [4]. In particular, the reactance terms are zero at the resonant frequency; therefore, the PTE at ω_o is reduced to

$$\eta_{\omega_o} = \frac{1}{1 + \frac{Q_L}{Q_r}\left[1 + \frac{1}{\sigma^2}\left(1 + \frac{Q_r}{Q_L}\right)^2\right]}. \quad (8)$$

Then the optimal load quality factor, Q_L^*, which is required to maximize η_{ω_o}, can be found from the condition $\partial\eta_{\omega_o} / \partial Q_L = 0$.

$$Q_L^* = \frac{Q_r}{\sqrt{1 + Q_t Q_r k^2}}. \quad (9)$$

By substituting (9) into (8), we can obtain the maximum PTE.

$$\begin{aligned} \eta_{\omega_o}^* &= \frac{1}{1 + \frac{1}{\sqrt{1+\sigma^2}}\left[1 + \left(\frac{1}{\sigma} + \sqrt{1 + \frac{1}{\sigma^2}}\right)^2\right]} \\ &= \frac{\sqrt{1 + Q_t Q_r k^2} - 1}{\sqrt{1 + Q_t Q_r k^2} + 1}. \end{aligned} \quad (10)$$

In (10), the PTE is proportional to σ, thus, to maximize the PTE, σ should be large. To increase σ, large Q and k are required. In particular, if the condition $\sigma^2 > 1$ is satisfied, then this is called a strong coupling regime [11]–[12]. In addition, in a magnetic-inductive channel, the subchannel close to ω_o has a high PTE.

The PTE η_ω indicates how much power is transmitted to the load resistor of the Rx coil at a frequency of ω; therefore, the received power can be expressed as $p_\omega \eta_\omega$, where p_ω is the transmitted power. Similarly, in the case of communication, information is also transferred to the load resistor of the Rx coil through the wireless channel. In this case, the received signal power can be expressed as $p_\omega |h_\omega|^2$, where $|h_\omega|^2$ is the channel gain of ω. In addition, the power transfer efficiency and the path loss of the MI channel for communication have a similar attenuation tendency, which is proportional to $1/d^6$. The relationship between the channel gain and the PTE (for a given value of ω) may, therefore, be defined by $\eta_\omega = |h_\omega|^2$ in the wireless information and power transfer system [21]. Then the capacity of subchannel i can, therefore, be expressed as $c_i = \log_2(1 + p_i \eta_i / N_0)$, where p_i is the power allocated to subchannel i and N_0 is the noise power of each subchannel.

III. Co-receiver Case

First, we consider the case of a co-receiver that combines a receiver for information detection (Rx-ID) and a receiver for power extraction (Rx-PE); that is, the Rx-ID and Rx-PE use the same resource. This means that it is possible to observe information and extract power simultaneously from the same signal. In the co-receiver case, we can find an OPA and provide the upper bound of achievable transferred power and capacity pairs. In addition, we propose a suboptimal algorithm that has low complexity.

1. OPA

Before proposing the OPA strategy, which considers the simultaneous transfer of information and power, we derive two power allocation strategies — one for maximizing transferred power and the other for maximizing information capacity.

Proposition 1. Total power allocation (TPA) on a subchannel that has the highest PTE, p_i^{TPA}, maximizes the transferred power for a given total available power. Then p_i^{TPA} is given by

$$\begin{aligned} p_{i_{\max}}^{\mathrm{TPA}} &= P_{\mathrm{S}} \quad \text{for } i_{\max} = \max_i \eta_i, \\ p_i^{\mathrm{TPA}} &= 0 \quad \text{otherwise}, \end{aligned} \tag{11}$$

where P_{S} is the total available power. The transferred power and capacity achieved by the TPA are defined as $\eta^{\mathrm{TPA}} = P_{\mathrm{S}}\eta_{\max}$ and $C^{\mathrm{TPA}} = \log_2(1 + P_{\mathrm{S}}\eta_{\max}/N_0)$, respectively.

Proof. The proof of Proposition 1 is simple and trivial; therefore, it is omitted here [20]. ■

Proposition 2. Water-filling power allocation (WFPA), p_i^{WF}, maximizes the sum of the capacities of the subchannels for a given total available power. Then p_i^{WF} is given by

$$p_i^{\mathrm{WF}} = \left(\frac{1}{\lambda_{\mathrm{WF}} \ln 2} - \frac{N_0}{\eta_i} \right)^+, \tag{12}$$

where we define $(x)^+ = \max(0, x)$ and λ_{WF} satisfies $\sum_{i=1}^{N} p_i^{\mathrm{WF}} = P_{\mathrm{S}}$. The transferred power and capacity achieved by the WFPA are defined as $\eta^{\mathrm{WF}} = \sum_{i=1}^{N} p_i^{\mathrm{WF}} \eta_i$ and $C^{\mathrm{WF}} = \sum_{i=1}^{N} \log_2(1 + p_i^{\mathrm{WF}} \eta_i / N_0)$, respectively.

Proof. The proof of Proposition 2 is well known; therefore, it is also omitted here [23]. ■

Proposition 1 suggests that the total available power must be allocated to the subchannel that has the highest PTE, to maximize the transferred power. However, this method cannot guarantee the required information capacity. On the other hand, Proposition 2 demonstrates that the WFPA can maximize the information capacity, but it does not consider the wireless power transfer. The analysis of Propositions 1 and 2 leads us to formulate the following optimization problem, whose objective is to maximize the transferred power while preserving the required information capacity within the total available power constraint, as follows:

$$\begin{aligned} \underset{\boldsymbol{p}}{\text{maximize}} \quad & \sum_{i=1}^{N} p_i \eta_i \\ \text{subject to (s.t.)} \quad & \sum_{i=1}^{N} c_i \geq C_{\mathrm{m}}, \\ & \sum_{i=1}^{N} p_i \leq P_{\mathrm{S}}, \\ & p_i \geq 0 \quad \text{for} \quad \forall i, \end{aligned} \tag{13}$$

where $\boldsymbol{p}$ is the set of power allocated to subchannels, such that $\boldsymbol{p} \triangleq (p_1, \cdots, p_N)$, and C_{m} is the required information capacity.

Theorem 1. If $C_{\mathrm{m}} > C^{\mathrm{TPA}}$, then the optimal solution of (13) is given by

$$p_i^* = \left(\frac{\mu^*}{(\lambda^* - \eta_i)\ln 2} - \frac{N_0}{\eta_i} \right)^+. \tag{14}$$

In addition, λ^* and μ^* satisfy the following conditions:

$$\sum_{i=1}^{N} \log_2 \left(1 + \frac{\left(\frac{\mu^*}{(\lambda^* - \eta_i)\ln 2} - \frac{N_0}{\eta_i} \right)^+ \cdot \eta_i}{N_0} \right) = C_{\mathrm{m}}, \tag{15}$$

$$\sum_{i=1}^{N} \left(\frac{\mu^*}{(\lambda^* - \eta_i)\ln 2} - \frac{N_0}{\eta_i} \right)^+ = P_{\mathrm{S}}; \tag{16}$$

otherwise, $p_i^* = p_i^{\mathrm{TPA}}$.

Proof. First, we find the OPA when $C_{\mathrm{m}} > C^{\mathrm{TPA}}$. The problem in (13) is a convex optimization problem. Therefore, to find an optimal solution, we consider its Lagrangian function given by (17), where λ and μ are non-negative Lagrange multipliers.

$$\Lambda(\boldsymbol{p}, \lambda, \mu) \triangleq \sum_{i=1}^{N} p_i \eta_i + \lambda \left(P_{\mathrm{S}} - \sum_{i=1}^{N} p_i \right) + \mu \left(\sum_{i=1}^{N} c_i - C_{\mathrm{m}} \right). \tag{17}$$

From the Lagrangian function, we define the following Karush–Kuhn–Tucker (KKT) conditions:

$$\frac{\mu}{\ln 2} \times \frac{\eta_i}{N_0} \times \frac{1}{1 + \frac{p_i \eta_i}{N_0}} + \eta_i - \lambda = 0, \tag{18}$$

$$\mu \left(\sum_{i=1}^{N} c_i - C_{\mathrm{m}} \right) = 0, \tag{19}$$

$$\lambda \left(P_{\mathrm{S}} - \sum_{i=1}^{N} p_i \right) = 0, \tag{20}$$

and $$\lambda \geq 0,\ \mu \geq 0,\ \boldsymbol{p} \succeq 0. \quad (21)$$

From the KKT condition (18), it is possible to find the optimal allocated power on each subchannel, which can then be represented as (14). Also, λ^* and μ^* can be obtained from complementary slackness conditions. For the maximum transferred power, both the required information capacity and the total available power constraints should be tight. This implies that the equalities $\sum_{i=1}^{N} \log_2(1+p_i^*\eta_i/N_0) - C_{\mathrm{m}} = 0$ and $P_{\mathrm{S}} - \sum_{i=1}^{N} p_i^* = 0$ should hold for positive numbers, λ and μ, in KKT conditions (19) and (20). Therefore, λ^* and μ^* satisfy (15) and (16).

When $C_{\mathrm{m}} \leq C^{\mathrm{TPA}}$, μ needs to be zero to satisfy (19) since $\sum_{i=1}^{N} c_i - C_{\mathrm{m}}$ is always greater than zero. The problem of (13) is the same as that of Proposition 1; thus, p_i^* is the same as p_i^{TPA}. ■

Proposition 3. The condition $\lambda \geq \eta_{\max}$ must hold so as to obtain a bounded optimal solution in (13).

Proof. Proposition 3 can be proved by a contradiction. Let us consider the Lagrangian dual function of (13), which is defined as

$$g(\lambda,\mu) = \max_{\boldsymbol{p}\succeq 0} \Lambda(\boldsymbol{p},\lambda,\mu). \quad (22)$$

Then, (22) can be simplified by discarding the constant terms related to λ and μ.

$$\max_{\boldsymbol{p}\succeq 0} \sum_{i=1}^{N} p_i(\eta_i - \lambda) + \mu \sum_{i=1}^{N} c_i. \quad (23)$$

Suppose that $\lambda < \eta_{\max}$. Then, the optimal value of (23) is unbounded when the p_i of the subchannel i with the maximum power transfer efficiency $\eta_{\max}$ goes to infinity. Thus, the assumption $\lambda < \eta_{\max}$ is a contradiction; hence, the proof is completed. ■

We can also find the upper bound of μ for a given λ. From the relation $P_{\mathrm{S}} > p_i$, $\mu_{\max}$ can be determined by $\ln 2 \times (\lambda - \eta_{\max}) \times (P_{\mathrm{S}} + N_0/\eta_{\max})$. Thus, μ lies in the interval $(0, \mu_{\max})$.

Since (13) is a convex optimization problem, μ^* and λ^* can be found by updating μ and λ jointly through a gradient algorithm. Therefore, p_i^* can also be found using an iterative method. The algorithm used to find p_i^* can be summarized in Algorithm 1. Here, α and β are step sizes that are sufficiently small to allow convergence, ε is given by a small positive number, and λ_{init} is the initial value of λ. If we denote I_α and I_β as the number of iterations for the convergence of μ and λ, respectively, then the computational complexity involved in finding p_i^* is $O(I_\alpha I_\beta)$.

Algorithm 1. Optimal power allocation.

Initialization: $k = 1, \lambda_k = \lambda_{\mathrm{init}}$
If $C_{\mathrm{m}} \leq C^{\mathrm{TPA}}$, set $p_i^* = p_i^{\mathrm{TPA}}$. Else,
Repeat
  Initialization: $k' = 1, \mu_{k'} = \mu_{\max}$
  Repeat
    Find p_i from (14) for all $i = 1, 2, \ldots, N$
    Update $\mu_{k'+1} = \mu_{k'} - \alpha\left(\sum_{i=1}^{N} c_i - C_{\mathrm{m}}\right)$
  Until $|\mu_{k'+1} - \mu_{k'}| \leq \varepsilon$
  Update $\lambda_{k+1} = \lambda_k - \beta\left(P_{\mathrm{S}} - \sum_{i=1}^{N} p_i\right)$
Until $|\lambda_{k+1} - \lambda_k| \leq \varepsilon$

2. Power Reallocation Algorithm (PRA)

In OPA, the exact value of p_i^* can be obtained if α and β are sufficiently small to allow convergence, but this makes the values of I_α and I_β large. Larger values of I_α and I_β significantly increase the computational complexity involved in calculating the exact value of p_i^*. As a result, it can be difficult to find p_i^* in real time. Thus, based on the analytical results in Section III-1, we propose a low-complexity PRA. This achieves near-optimal performance, while substantially reducing the computational complexity so that power can be allocated in real time.

In the OPA, μ^* and λ^* should be obtained jointly using a gradient algorithm to find p_i^*. However, in the PRA, μ and λ are found separately. First, the values of μ and λ are initialized as $\mu_{\max}$ and λ_{init}. Secondly, μ is found separately by the gradient algorithm for the given value of λ_{init}. In this step, the required information capacity is guaranteed because μ and λ_{init} satisfy condition (15), but P_{S} is not used fully. Therefore, in the third step, λ is also found by the gradient algorithm for the determined value of μ to satisfy condition (16). The water level $(\mu/(\lambda - \eta_i)\ln 2)$ in (14) increases as λ is updated by the gradient algorithm, so the remaining available power can be used fully. However, in this step, the achieved capacity is greater than the required information capacity C_{m}, so loss occurs in transferred power because supporting the exact value of C_{m} can increase transferred power. Thus, the fourth step is needed to satisfy both (15) and (16) by reassigning the allocated power; the process of which is described as follows:

1. A transmitter finds the subchannel $i_{\min}$ that achieves the minimum capacity among those subchannels whose capacity is greater than zero, such that $c_{\min} = \min_i c_i$ for $c_i > 0$.
2. The transmitter eliminates the allocated power $p_{i_{\min}}$ in subchannel $i_{\min}$ and reallocates $p_{i_{\min}}$ to the subchannel $i_{\max}$ that has the highest PTE, $\eta_{\max}$.

http://dx.doi.org/10.4218/etrij.14.0114.0161

In general, the subchannel $i_{\max}$ uses a resonant frequency as its central frequency. If the sum capacity of the subchannels after the reallocation of power is still greater than C_{m}, then the aforementioned fourth step is repeated. Otherwise, $p_{i_{\min}}$ is reduced by half to find the value that exactly guarantees C_{m}. Thus, $p_{i_{\min}}$ can be determined using a bisection algorithm. The fourth step is terminated when C_{m} is guaranteed accurately or the total available power is allocated to subchannel $i_{\max}$; that is when $\left|\sum_{i=1}^{N} c_i - C_{\mathrm{m}}\right| \le \varepsilon$ or $p_{i_{\max}} = P_{\mathrm{S}}$, respectively. The case of $p_{i_{\max}} = P_{\mathrm{S}}$ occurs when C_{m} is sufficiently small, so C_{m} can be guaranteed even though the total available power is allocated to subchannel $i_{\max}$. The process of the PRA is summarized in Algorithm 2.

Algorithm 2. Power reallocation algorithm.

1: Initialization: $k = 1, \lambda_k = \lambda_{\text{init}}, k' = 1, \mu_{k'} = \mu_{\max}$
2: **Repeat**
3: Find p_i from (14) for all $i = 1, 2, \ldots, N$
4: Update $\mu_{k'+1} = \mu_{k'} - \alpha\left(\sum_{i=1}^{N} c_i - C_{\mathrm{m}}\right)$
5: **Until** $|\mu_{k'+1} - \mu_{k'}| \le \varepsilon$
6: **Repeat**
7: Find p_i from (14) for all $i = 1, 2, \ldots, N$
8: Update $\lambda_{k+1} = \lambda_k - \beta\left(P_{\mathrm{S}} - \sum_{i=1}^{N} p_i\right)$
9: **Until** $|\lambda_{k+1} - \lambda_k| \le \varepsilon$
10: **Repeat**
11: Find the subchannel $i_{\min}$ and set $p_{\text{temp}} = p_{i_{\min}}$
12: **Repeat**
13: Set $p_{i_{\min}} = p_{i_{\min}} - p_{\text{temp}}$ and $p_{i_{\max}} = p_{i_{\max}} + p_{\text{temp}}$
14: Set $p_{\text{temp}} = p_{\text{temp}} / 2$
15: **Until** $\sum_{i=1}^{N} c_i \ge C_{\mathrm{m}}$
16: **Until** $\left|\sum_{i=1}^{N} c_i - C_{\mathrm{m}}\right| \le \varepsilon$ or $p_{i_{\max}} = P_{\mathrm{S}}$

In short, the PRA finds the minimum size of B that guarantees C_{m} by eliminating $p_{i_{\min}}$ in subchannel $i_{\min}$. At the same time, the transferred power is efficiently increased while ensuring a minimum loss of capacity by reallocating $p_{i_{\min}}$ to subchannel $i_{\max}$. In addition, the computational complexity of the PRA is $O(I_\alpha + I_\beta + N\log_2 N)$, where $N\log_2 N$ is very small compared with I_α or I_β. This indicates that the PRA achieves a significant reduction in complexity compared with $O(I_\alpha I_\beta)$ when calculating p_i^* exactly and that it allows operation in real time.

We now compare four methods, TPA, WFPA, OPA, and PPA, to explain the benefits of the proposed solutions. Figure 2

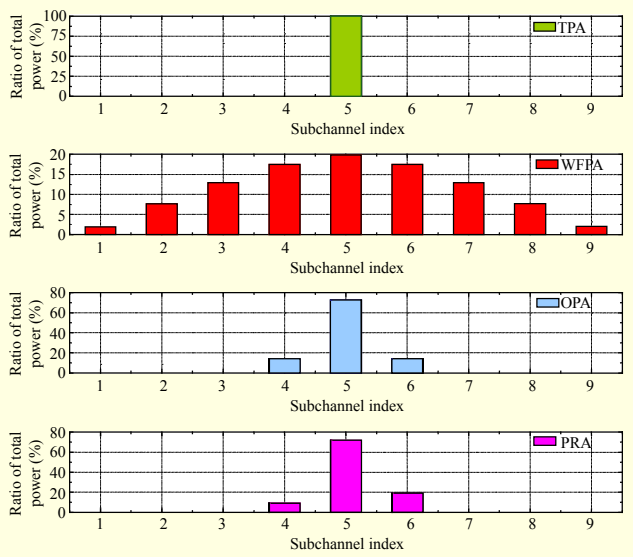

Fig. 2. Allocated powers of TPA, WFPA, OPA, and PRA.

shows the allocated powers obtained using the four methods. When the TPA is used to allocate power, the total available power is allocated to only the subchannel with the highest PTE. This approach leads to a maximum transferred power using a minimum bandwidth. On the other hand, the WFPA uses a broader bandwidth than the TPA to achieve the maximum capacity. When the WFPA is used to obtain p_i^{WF}, the water level $(1/\lambda_{\mathrm{WF}}\ln 2)$ is the same for all subchannels and more power is allocated to subchannels that have a higher PTE. Conversely, the OPA can be executed by controlling the water level of each subchannel. When the OPA is used to obtain p_i^*, the water level $(\mu^*/(\lambda^* - \eta_i)\ln 2)$ varies for each subchannel. The subchannel with a higher PTE, therefore, has a higher water level. Thus, compared with p_i^{WF}, more power is allocated to the subchannel with higher PTE, while less power is allocated to the subchannel with lower PTE. This means that the OPA uses the minimum bandwidth needed to ensure the required information capacity by reducing the allocated power in the subchannel with lower PTE. At the same time, the OPA maximizes the transferred power by allocating more power to the subchannel with higher PTE instead of the subchannel with lower PTE. Also, we show that the allocated power of the PRA is almost the same as that of the OPA. This indicates that the PRA achieves a near-OPA with a significant reduction in complexity, compared with the OPA. The PTE-capacity (η-C) regions that describe all achievable PTE and capacity pairs can be expressed as follows:

$$R_{\eta-C}(\boldsymbol{p}) \triangleq \left\{(\eta, C) : \eta \le \sum_{i=1}^{N} p_i \eta_i,\ C \le \sum_{i=1}^{N} c_i, \sum_{i=1}^{N} p_i \le P_{\mathrm{S}}, \boldsymbol{p} \succeq 0\right\}. \quad (24)$$

IV. Separated-Receiver Case

It is difficult to implement a co-receiver practically; thus, we consider a separated-receiver case that separates an Rx-ID and an Rx-PE for practical consideration. In the separated-receiver case, the Rx-ID and Rx-PE observe information and extract power separately from different resources. Here, we propose two heuristic power allocation algorithms based on frequency division and time division.

1. Power Allocation Based on Frequency Division (PA-FD)

Information and power can be transferred through different frequencies. In general, it is best to use only the subchannel that has the largest PTE for transferring power. Thus, we use the subchannel $i_{\max}$ for transferring power and use other subchannels for transferring information. When a PA-FD is used in a separated-receiver case, we can formulate the following optimization problem:

$$\begin{aligned} \underset{\boldsymbol{p}}{\text{maximize}} \quad & p_{i_{\max}}\eta_{i_{\max}} \\ \text{subject to (s.t.)} \quad & \sum_{i=1,i\neq i_{\max}}^{N} c_i \geq C_{\mathrm{m}}, \\ & \sum_{i=1}^{N} p_i \leq P_{\mathrm{S}}, \\ \text{and} \quad & p_i \geq 0 \quad \text{for} \quad \forall i. \end{aligned} \tag{25}$$

Theorem 2. If we assume that C_{m} is sufficiently small, such that $C_{\mathrm{m}} << C^{\mathrm{WF}}$, then the solution of (25) is given by

$$p_i^{\mathrm{FD}} = \left(\frac{\mu}{\lambda \ln 2} - \frac{N_0}{\eta_i}\right)^{+}, \tag{26}$$

$$p_{i_{\max}}^{\mathrm{FD}} = P_{\mathrm{S}} - \sum_{i=1,i\neq i_{\max}}^{N} p_i^{\mathrm{FD}}. \tag{27}$$

Proof. Since the problem (25) is a convex optimization problem, we consider its Lagrangian function, given by (28), where λ and μ are non-negative Lagrange multipliers.

$$\Lambda(\boldsymbol{p},\lambda,\mu) \triangleq p_{i_{\max}}\eta_{i_{\max}} + \lambda\left(P_{\mathrm{S}} - \sum_{i=1}^{N} p_i\right) + \mu\left(\sum_{i=1,i\neq i_{\max}}^{N} c_i - C_{\mathrm{m}}\right). \tag{28}$$

By differentiating $\Lambda(\boldsymbol{p},\lambda,\mu)$ with respect to p_i, p_i can be obtained as (26). To find $p_{i_{\max}}$, we can rewrite (28) as $\Lambda(\boldsymbol{p}, \lambda) \triangleq p_{i_{\max}}(\eta_{i_{\max}} - \lambda) + \lambda(P_{\mathrm{S}} - \sum_{i=1, i\neq i_{\max}}^{N} p_i)$ by eliminating constant terms. In addition, the Lagrangian dual function of (25) can be given by $g(\lambda) = \max_{\boldsymbol{p}\succeq 0} \Lambda(\boldsymbol{p},\lambda)$. Here, the condition $(\eta_{i_{\max}} - \lambda) \leq 0$ should be met so that $g(\lambda)$ has a bounded value. Otherwise, $g(\lambda)$ is unbounded as $p_{i_{\max}}$ tends to infinity. In addition, the dual problem of (25) is defined as $\min_{\lambda\succeq 0} g(\lambda)$. It has a zero duality gap, so the following equality should be satisfied for the optimal primal and dual solutions: $p_{i_{\max}}^{*}\left(\eta_{i_{\max}} - \lambda^{*}\right) = 0$.

Then, the dual problem can be rewritten as follows:

$$\begin{aligned} \underset{\lambda}{\text{minimize}} \quad & \lambda\left(P_{\mathrm{S}} - \sum_{i=1,i\neq i_{\max}}^{N} p_i\right) \\ \text{subject to (s.t.)} \quad & \eta_{i_{\max}} - \lambda \leq 0, \\ & \lambda \geq 0. \end{aligned} \tag{29}$$

Thus, from (29), the solution of λ is $\eta_{i_{\max}}$, and $p_{i_{\max}}$ can be obtained as (27). ■

The PA-FD implies that the power is allocated to subchannels for transferring information at first to guarantee C_{m}, and then the remaining power is allocated to the subchannel for transferring power. When $C_{\mathrm{m}} = 0$, the PA-FD is the same as TPA; thereby, maximizing the transferred power. However, the PA-FD cannot achieve the maximum information capacity C^{WF} even though total power is used for transferring information, because the subchannel $i_{\max}$ cannot be used for transferring information. Then, the η-C regions of the PA-FD can be expressed as follows:

$$R_{\eta-\mathrm{C}}^{\mathrm{FD}}(\boldsymbol{p}) \triangleq \left\{ \begin{array}{l} (\eta, C): \eta \leq p_{i_{\max}}^{\mathrm{FD}}\eta_{i_{\max}}, \\ C \leq \sum_{i=1,i\neq i_{\max}}^{N} \log_2\left(1 + \frac{p_i^{\mathrm{FD}}\eta_i}{N_0}\right), \sum_{i=1}^{N} p_i \leq P_{\mathrm{S}}, \boldsymbol{p}\succeq 0 \end{array} \right\}. \tag{30}$$

2. Power Allocation Based on Time Division (PA-TD)

Information and power can be transferred at different moments in a time slot. It is best to use WFPA for transferring information, whereas it is best to use TPA for transferring power. Therefore, a PA-TD can be defined simply by using WFPA and TPA. Let ρ, $0 \leq \rho \leq 1$, denote the ratio of transmission time allocated for transferring information. Then the WFPA is used firstly for transferring information until $\rho C^{\mathrm{WF}} = C_{\mathrm{m}}$. After that, the TPA is used for transferring power during the remaining time $(1 - \rho)$. Then the transferred power becomes $(1 - \rho)\eta^{\mathrm{TPA}}$. The PA-TD, therefore, ensures that for any given portion of a time slot, the initial part is used for the transfer of information until C_{m} is guaranteed and the remaining part is used for the transfer of power. When $C_{\mathrm{m}} = 0$ and $\rho = 0$, the PA-TD can achieve the maximum transferred power η^{TPA}. Also, it can achieve the maximum information capacity C^{WF} when $\rho = 1$. This means that the PA-TD is more efficient than the PA-FD as C_{m} approaches C^{WF}. Then the η-C regions of the PA-TD can be expressed as follows:

$$R_{\eta-C}^{\mathrm{TD}}(\boldsymbol{p}) \triangleq \left\{ \begin{array}{l} (\eta, C): \eta \le (1-\rho) P_{\mathrm{S}} \eta_{i_{\max}}, \\ C \le \rho \sum_{i=1}^{N} \log_2 \left(1 + \frac{p_i^{\mathrm{WF}} \eta_i}{N_0} \right), \sum_{i=1}^{N} p_i \le P_{\mathrm{S}}, \boldsymbol{p} \succeq 0 \end{array} \right\}. \quad (31)$$

V. Simulation Results and Discussion

In our simulations, we consider identical Tx and Rx coils with a radius of 0.3 m and an internal resistance of 0.5 Ω. The self-inductance of the coils is chosen depending on the value of Q, such as $L = Q_{\mathrm{r}}/\omega_{\mathrm{o}}$. In addition, the self-capacitance of the coils is chosen depending on the value of self-inductance, such as $C = 1/\omega_{\mathrm{o}}^2 L$, to make the two coils resonate at the same frequency of 10 MHz. Also, we use the optimal load quality factor Q_{L}^* at all distances. We set P_{S} to 1 W, so the transferred power can simply be considered to be the PTE. The bandwidth is 250 kHz, and there are nine subchannels. We assume that the total noise power is equal to one; thus, the noise power of each subchannel is $N_0 = 1/9$. For comparative purposes, we use the EPA scheme, which allocates power equally to all subchannels, as a conventional scheme.

Figure 3 shows the PTE η versus frequency. To verify the magnetic-inductive channel, we perform both circuit and EM simulations using the Agilent ADS and the Ansoft HFSS, respectively. As Q increases, the strong resonance between the Tx and Rx coils occurs. As a result, subchannels near ω_{o} have higher PTE and the variation of PTE among subchannels becomes large. On the other hand, as k increases, the coupling strength between the Tx and Rx coils becomes large. Consequently, the PTE of all subchannels increases generally, which relieves the variation of PTE among subchannels. This means that the magnetic-inductive channel has different characteristics depending on the values of Q and k. There are

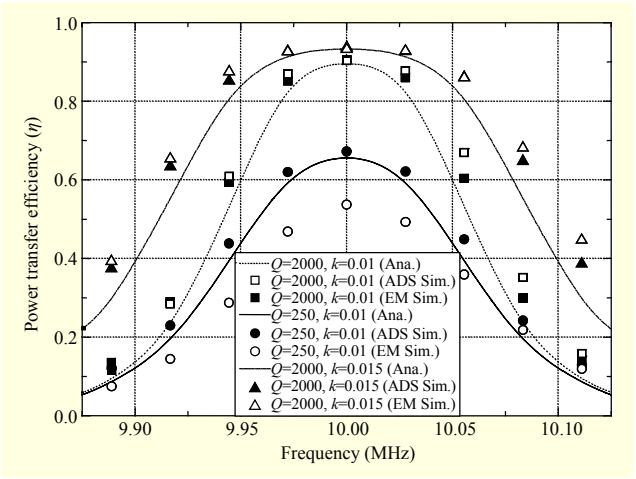

Fig. 3. η vs. frequency.

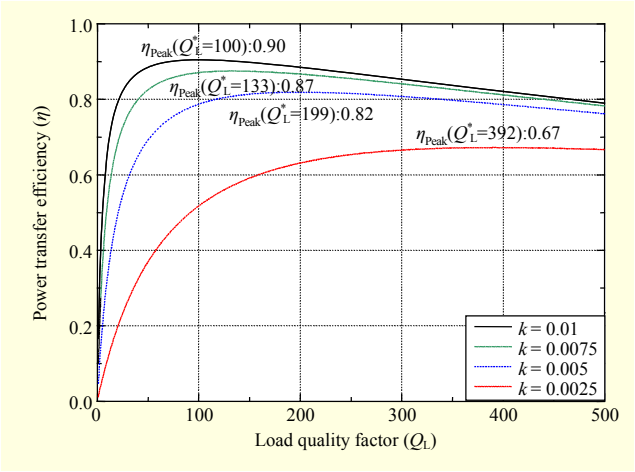

Fig. 4. η vs. Q_{L}.

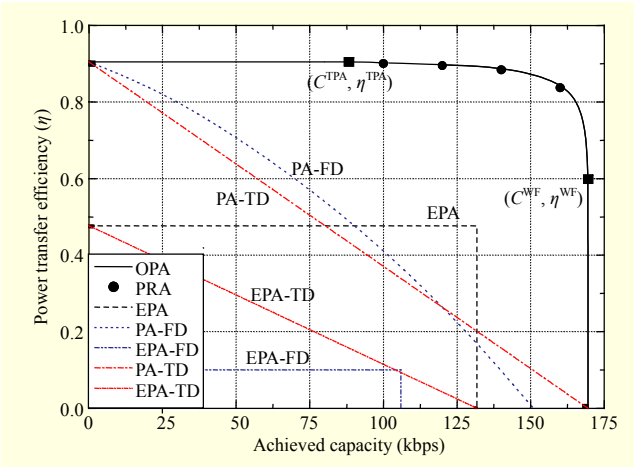

Fig. 5. η vs. C when $k = 0.01$ and $Q = 2{,}000$.

some differences between the analytical and simulation results, as the subchannels are apart from ω_{o} because we approximated $j\omega L_{\mathrm{t}} + 1/j\omega C_{\mathrm{t}} \approx j2(\Delta\omega)(Q_{\mathrm{t}})r_{\mathrm{lt}}$ and $j\omega L_{\mathrm{r}} + 1/j\omega C_{\mathrm{r}} \approx j2(\Delta\omega)(Q_{\mathrm{r}})r_{\mathrm{lr}}$ in (4) using the first-order Taylor series expansion. However, the analytical results are relatively well-matched to both simulation results.

Figure 4 shows the PTE η versus the load quality factor Q_{L} for different k. At a given k, there is an optimal load quality factor where the maximum η is achieved. For example, the maximum η at $Q_{\mathrm{L}} = 100$ is 0.90 when $k = 0.01$, which is indicated as $\eta_{\mathrm{Peak}}(Q_{\mathrm{L}}^* = 100) : 0.90$ in Fig. 4. Since the optimal load quality factor is inversely proportional to k in (9), the value of Q_{L}^* is small for large k.

Figure 5 shows the capability in power and information transfer. In η-C regions, the boundary point $(C^{\mathrm{TPA}}, \eta^{\mathrm{TPA}})$ can be obtained using TPA. Another boundary point, $(C^{\mathrm{WF}}, \eta^{\mathrm{WF}})$, can be obtained using WFPA. Here, η^{TPA} is the maximum achievable PTE, which can be obtained when $C \le C^{\mathrm{TPA}}$.

Similarly, C^{WF} is the maximum achievable capacity, which can be obtained when $\eta \le \eta^{WF}$. The η achieved by OPA lies on the boundary line between two boundary points; for example, $\eta^{WF} \le \eta \le \eta^{TPA}$ and $C^{TPA} \le C \le C^{WF}$; however, its exact position depends on the required information capacity constraint. In the η-C regions, there are four circular points that indicate the η obtained using PRA. These points are close to the boundary of the η-C regions, which implies that the PRA achieves near-optimal η while reducing the computational complexity considerably. In addition, when C_m is small, the PRA uses a narrow bandwidth. So, power is allocated intensively on the subchannels with higher PTE and that are close to ω_o. On the other hand, the PRA uses a broad bandwidth at larger values of C_m. So, power is allocated to even the subchannels with lower PTE, which are far from ω_o, to guarantee C_m. As a result, the η of the PRA decreases as C_m increases. PA-TD can use all subchannels for transferring both information and power, and can control ρ adaptively depending on C_m. On the other hand, PA-FD cannot use the subchannel i_{max} for transferring information although large C_m is required. This means that the PA-FD is inefficient when C_m is large; as a result, the η of the PA-FD is lower than that of the PA-TD as C_m increases. EPA cannot allocate power to subchannels while considering C_m, so the η of the EPA is constant regardless of the achieved capacity. On the other hand, the PA-FD and PA-TD can use power efficiently for transferring power rather than information when C_m is small. As a result, the PA-FD and PA-TD achieve higher η than the EPA when the achieved capacity is small.

Figure 6 shows the PTE η versus the quality factor Q when $k = 0.01$ and $C_m = 80$ kbps. The PTE of subchannels becomes higher as Q increases, so the performance of all schemes increases. The PTE among subchannels is relatively constant at small Q, so the proposed algorithms allocate power to all subchannels evenly, which is similar to EPA. However, the PTE of subchannels varies significantly as Q increases, so power is allocated intensively to the subchannels near ω_o. Consequently, the PA-FD, PA-TD, and OPA all achieve higher η than the EPA for large Q. In addition, the proposed algorithms can perform power allocation adaptively when the PTE of subchannels is changed with the variation of Q. Therefore, the η of the proposed algorithms is improved more rapidly than that of the EPA schemes as Q increases.

Figure 7 shows the PTE η versus the coupling coefficient k when $Q = 2{,}000$ and $C_m = 80$ kbps. The PTE of all subchannels becomes better as k increases, which causes a little variation of PTE among subchannels. This indicates that the performance gain that can be achieved by the proposed algorithms becomes small; consequently, the η of EPA becomes higher than that of PA-FD and PA-TD for large k. The EPA-FD cannot adapt to the variation of channel quality or C_m, while EPA-TD can

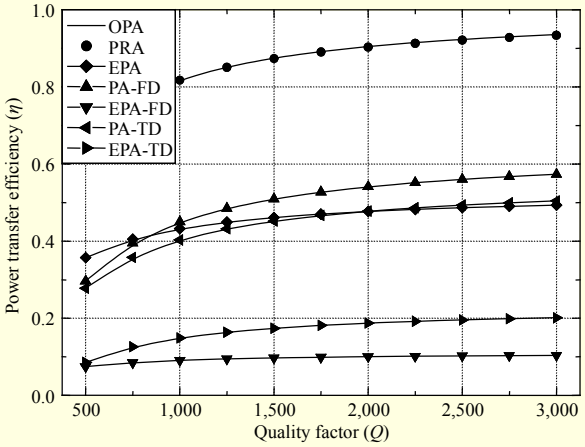

Fig. 6. η vs. Q when $k = 0.01$ and $C_m = 80$ kbps.

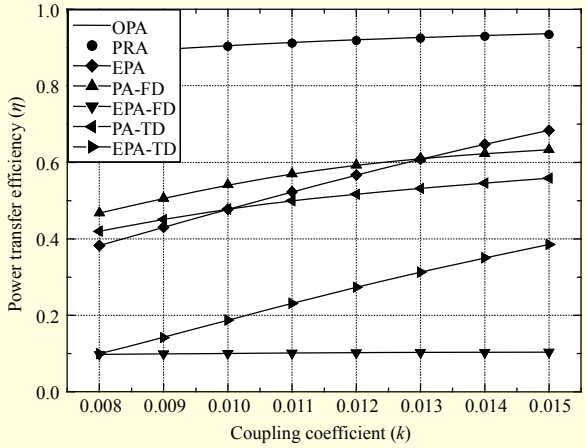

Fig. 7. η vs. k when $Q = 2{,}000$ and $C_m = 80$ kbps.

adjust the ratio of transmission time, ρ, adaptively depending on the situation. Consequently, there is little variation in η in the EPA-FD; however, η increases as k increases in the EPA-TD. Also, we can show that the proposed algorithms can achieve higher η than the EPA schemes in both the co-receiver and the separated-receiver cases, in Figs. 6 and 7.

VI. Conclusion

In this paper, we considered the maximization of transferred power while ensuring the required information capacity within the total available power constraint in a wireless information and power transfer system. We constructed an equivalent circuit model for our magnetic resonance–based system and provided a magnetic-inductive channel model. Based on a formulated convex optimization problem, we derived an optimal power allocation (OPA) strategy in the case of the co-receiver. In addition, we found the conditions for the existence

and boundedness of the OPA. To reduce the computational complexity of the OPA, we also proposed a low-complexity power reallocation algorithm. For practical consideration, we also proposed two heuristic algorithms in the case of the separated receiver. In our simulation results, we verified the characteristic of the magnetic-inductive channel. Also, we provided the η-C regions to compare the performance of the proposed algorithms with that of the OPA. In short, we provided not only a theoretical performance bound of achievable transferred power and capacity pairs but also the algorithms that can be implemented in real time. For further works, it is necessary to address some practical issues, such as the effect of noise, the experimental verification of the MI channel, and electromagnetic compatibility with other existing systems.

References

[1] T. Yamazaki, "The Ubiquitous Home," *Int. J. Smart Home*, vol. 1, no. 1, Jan. 2007, pp. 17–22.

[2] I.F. Akyildiz and E.P. Stuntebeck, "Wireless Underground Sensor Networks: Research Challenges," *Ad Hoc Netw. J.*, vol. 4, no. 6, Nov. 2006, pp. 669–686.

[3] L. Li, M.C. Vuran, and I.F. Akyildiz, "Characteristics of Underground Channel for Wireless Underground Sensor Networks," *IFIP Mediterranean Ad Hoc Netw. Workshop*, Corfu, Greece, June 12–15, 2007, pp. 92–99.

[4] Z. Sun and I.F. Akyildiz, "Magnetic Induction Communications for Wireless Underground Sensor Networks," *IEEE Trans. Antennas Propag.*, vol. 58, no. 7, July 2010, pp. 2426–2435.

[5] E. Shamonina et al., "Magneto-Inductive Waves in One, Two, and Three Dimensions," *J. Appl. Phys.*, vol. 92, no. 10, Nov. 2002, pp. 6252–6261.

[6] R.R.A. Syms, I.R. Young, and L. Solymar, "Low-Loss Magneto-Inductive Waveguides," *J. Phys. D: Appl. Phys.*, vol. 39, no. 18, Sept. 2006, pp. 3945–3951.

[7] Z. Sun and I.F. Akyildiz, "Deployment Algorithms for Wireless Underground Sensor Networks Using Magnetic Induction," *IEEE Global Telecommun. Conf.*, Miami, FL, USA, Dec. 6–10, 2010, pp. 1–5.

[8] H. Jiang and Y. Wang, "Capacity Performance of an Inductively Coupled Near Field Communication System," *IEEE Antennas Propag. Society Int. Symp.*, San Diego, CA, USA, July 5–11, 2008, pp. 1–4.

[9] J.I. Agbinya and M. Masihpour, "Power Equations and Capacity Performance of Magnetic Induction Body Area Network Nodes," *Broadband Biomed. Commun.*, Malaga, Spain, Dec. 15–17, 2010, pp. 1–6.

[10] U. Azad, H.C. Jing, and Y.E. Wang, "Link Budget and Capacity Performance of Inductively Coupled Resonant Loops," *IEEE Trans. Antennas Propag.*, vol. 60, no. 5, May 2012, pp. 2453–2461.

[11] A. Kurs et al., "Wireless Power Transfer via Strongly Coupled Magnetic Resonances," *Sci. Mag.*, vol. 317, no. 5834, July 6, 2007, pp. 83–86.

[12] A. Karalis, J.D. Joannopoulos, and M. Soljacic, "Efficient Wireless Non-radiative Mid-range Energy Transfer," *Ann. Phys.*, vol. 323, no. 1, Jan. 2008, pp. 34–48.

[13] C.-J. Chen et al., "A Study of Loosely Coupled Coils for Wireless Power Transfer," *IEEE Trans. Circuits Syst. II, Exp. Briefs*, vol. 57, no. 7, July 2010, pp. 536–540.

[14] M. Kiani and M. Ghovanloo, "The Circuit Theory behind Coupled-Mode Magnetic Resonance-Based Wireless Power Transmission," *IEEE Trans. Circuits Syst. I, Reg. Papers,* vol. 59, no. 9, Sept. 2012, pp. 2065–2074.

[15] A. Kurs, R. Moffatt, and M. Soljacic, "Simultaneous Mid-range Power Transfer to Multiple Devices," *Appl. Phys. Lett.*, vol. 96, no. 4, Jan. 2010, p. 044102.

[16] B.L. Cannon et al., "Magnetic Resonant Coupling as a Potential Means for Wireless Power Transfer to Multiple Small Receivers," *IEEE Trans. Power Electron.*, vol. 24, no. 7, July 2009, pp. 1819–1825.

[17] J. Casanova, Z.N. Low, and J. Lin, "A Loosely Coupled Planar Wireless Power System for Multiple Receivers," *IEEE Trans. Ind. Electron.*, vol. 56, no. 8, Aug. 2009, pp. 3060–3068.

[18] J. Kim et al., "Efficiency Analysis of Magnetic Resonance Wireless Power Transfer with Intermediate Resonant Coil," *IEEE Antennas Wireless Propag. Lett.*, vol. 10, May 2011, pp. 389–392.

[19] L.R. Varshney, "Transporting Information and Energy Simultaneously," *IEEE Int. Symp. Inf. Theory*, Toronto, ON, USA, July 6–11, 2008, pp. 1612–1616.

[20] R. Zhang and C.K. Ho, "MIMO Broadcasting for Simultaneous Wireless Information and Power Transfer," *IEEE Global Telecommun. Conf.*, Houston, TX, USA, Dec. 5–9, 2011, pp. 1–5.

[21] P. Grover and A. Sahai, "Shannon Meets Tesla: Wireless Information and Power Transfer," *IEEE Int. Symp. Inf. Theory*, Austin, TX, USA, June 13–18, 2010, pp. 2363–2367.

[22] Z. Wang and G.B. Giannakis, "Wireless Multicarrier Communications," *IEEE Signal Process. Mag.*, vol. 17, no. 3, May 2000, pp. 29–48.

[23] T.M. Cover and J.A. Thomas, *Elements of Information Theory*, New York, USA: John Wiley & Sons Inc., 1991.

Kisong Lee received his BS degree in electrical engineering from the Information and Communications University, Daejeon, Rep. of Korea, in 2007 and his MS and PhD degrees in electrical engineering from the Korea Advanced Institute of Science and Technology, Daejeon, Rep. of Korea, in 2009 and 2013, respectively. He is currently with the Electronics and Telecommunications Research Institute as a researcher. His research interests include femtocell networks, self-organizing networks, radio resource management, magnetic induction communication, energy harvesting, and wireless power transfer.

Dong-Ho Cho received his PhD degree in electrical engineering from the Korea Advanced Institute of Science and Technology (KAIST), Daejeon, Rep. of Korea, in 1985. From 1987 to 1997, he was a professor at the Department. of Computer Engineering, Kyunghee University, Seoul, Rep. of Korea. Since 1998, he has been a professor at the Department of Electrical Engineering, KAIST, and he was a director of the KAIST Institute for Information Technology Convergence from 2007 to 2011. He has been a director of the KAIST Online Electric Vehicle Project since 2009, and he has been serving as a head of The Cho Chun Shik Graduate School for Green Transportation since 2010. He was also an IT Convergence Campus vice president of KAIST from 2011 to 2013. His research interests include mobile communication, Online Electric Vehicle systems based on wireless power transfer, and bio informatics.